PRACE INSTYTUTU ODLEWNICTWA
TRANSACTIONS OF FOUNDRY RESEARCH INSTITUTE

Volume LVI Year 2016 Number 3

Microstructure of selected 7xxx series aluminum alloys obtained by semi-continuous casting

Mikrostruktura wybranych stopów aluminium otrzymanych na drodze półciągłego odlewania

Zofia Kwak[1], Aldona Garbacz-Klempka[1], Małgorzata Perek-Nowak[2]

[1] AGH Akademia Górniczo-Hutnicza im. Stanisława Staszica w Krakowie, Wydział Odlewnictwa, ul. Reymonta 23, 30-059 Kraków

[2] AGH Akademia Górniczo-Hutnicza im. Stanisława Staszica w Krakowie, Wydział Metali Nieżelaznych, al. Mickiewicza 30, 30-059 Kraków

[1] AGH – University of Science and Technology, Faculty of Foundry Engineering, ul. Reymonta 23, 30-059 Kraków, Poland

[2] AGH – University of Science and Technology, Faculty of Non-Ferrous Metals, al. Mickiewicza 30, 30-059 Kraków, Poland

E-mail: kwakzosia@gmail.com

Received: 8.07.2016. Accepted in revised form: 30.09.2016.

DOI: 10.7356/iod.2016.16

Abstract

The study was conducted for two selected 7xxx series aluminum alloys according to PN-EN 573-3:2010 – Polish version. The analysis of ingots was carried out on 7003, 7003S and 7010, 7010K alloys with a similar ratio of zirconium content. Symbols S and K are our internal modifications, still compatible with the standard. The ingots were made by semi-continuous casting. Aluminum alloys of this series, with improved properties, are intended for plastic-processing.

The aim of this publication is to show how the microstructure of ingots is being formed during semi-continuous casting. The chemical profiles of ingots were determined using optical emission spectroscopy. Chemical analysis in micro-areas with evaluation by scanning electron microscope SEM with EDS analyzer was performed and the distribution of chemical elements in the microstructures are also presented. An XRD detector was used to show specific phases in the alloys.

The grains are formed in a particular way during crystallization. In the middle of the ingot – further away from the crystallizer – the grains are larger. Semi-continuous casting together with homogenization enables the production of ingots with uniform cross sections as can be seen in the paper.

Keywords: Al-Zn-Mg-Cu alloys, DC casting, quality of ingots, microstructure, micro-structural analysis with scanning electron microscope with included SEM-EDS, phase composition by X-Ray Diffraction (XRD)

Streszczenie

Badania prowadzono dla dwóch wybranych stopów aluminium serii 7xxx zgodnie z PN-EN 573-3:2010 – wersja polska. Ocenę wlewków prowadzono na stopach 7003, 7003S oraz 7010, 7010K o zbliżonej zawartości cyrkonu. Oznaczenia S i K to modyfikacja wewnętrzna, nadal zgodna z normą. Wlewki wykonane zostały na drodze odlewania półciągłego. Stopy aluminium tej serii, o podwyższonych właściwościach, przeznaczone są do przeróbki plastycznej.

Celem publikacji jest pokazanie, w jaki sposób kształtuje się mikrostruktura wlewków podczas półciągłego odlewania. Profile chemiczne wlewków wykonano przy wykorzystaniu optycznej spektroskopii emisyjnej. Wykonano również badania mikrostruktury wraz z analizą składu chemicznego w mikroobszarach z wykorzystaniem mikroskopu skaningowego (SEM) z analizatorem EDS oraz zaprezentowano rozkład pierwiastków na mikrostrukturach. Do wskazania konkretnych faz w stopach zastosowano detektor XRD.

Ziarna podczas krystalizacji wlewków kształtują się w charakterystyczny sposób. Średnica ziaren zwiększa się w kierunku środka wlewka, wraz z oddalaniem się od krystalizatora. Półciągłe odlewanie w połączeniu z homogenizacją umożliwia wykonanie wlewków o jednolitym przekroju poprzecznym, co zostało zaprezentowane w pracy.

Słowa kluczowe: stopy Al-Zn-Mg-Cu, odlewanie półciągłe, jakość wlewków, mikrostruktura, skład fazowy badany dyfrakcją rentgenowską SEM-EDS, XRD

1. Introduction

Aluminum, in spite of it being perceived as a new material, holds a key position in industry. Its role in the development of advanced technologies continues to grow, according to the latest publications of reports from manufacturing and sales. Aluminum occupies a key position among non-ferrous metals – ahead of copper – both in the production area, as well as being important to the global economy [1,2].

The last decade brought great progress in the production of aluminum and the use of new techniques in casting, forming, welding and modification of its surface. This development was intended to improve the structural integrity of aluminum alloys. They are used in the aviation industry, aerospace, automotive industry, electrical engineering, in parts of electrical machinery and devices, in the construction sector, as well as in the fields of metallurgy and many others. The mentioned alloys are often used for aesthetic purposes as well. Aluminum to a large extent owes its attractiveness to favorable casting properties, (including good fluidity, high impermeability, and low casting shrinkage), the possibility of using a combination of alloying elements, improvements in the refining processes and the possibility of modification of its alloys [3−6].

Trends caused by the directives of the European Union, associated with the gradual reduction of CO_2 emissions to the atmosphere, exerts pressure on industries that affect the increase in the average temperature of the Earth by greenhouse gas emissions. This often leads to the need to modify the previously used solutions, and sometimes to adopt complete change. These trends are particularly noticeable in the field of materials science, where modern materials are being developed. The recipients of the developed materials are mainly automotive, rail and aviation industries. Therefore, this also applies to aluminum alloys [2,7].

1.1. History and Process Description of Direct Chill (DC) Casting

Direct chill casting of aluminum alloys, commonly known as DC casting was developed in parallel by VAW from Germany and Alcoa (USA) at the beginning of 1830s. In the 1950s ingots cast that way were used for the production of large elements for aviation, shipbuilding and transport industries. Aluminum has also been used for the production of cans for drinks since the 1960s. It would have been impossible nowadays to use alloys with a high ratio of magnesium like the ones from series 2xxx and 7xxx, for the production of large parts for aviation without ingots produced in the process of semi-continuous casting. It also applies to plates from alloys 3xxx and 5xxx meant for cans. In 1956 the first Australian castings were made using this method, at Comal co Aluminum Limited's Bell Bay smelter [10−11].

At present it is the most important process of casting aluminum, even though it is not a new technology. It forms the material with high quality that is required for later extrusion, rolling or re-melting. Technology of semi-continuous casting is being used as well in the processes of casting copper, zinc or magnesium [10].

The semi-continuous casting method enables production of ingots with uniform cross-section. Firstly, the liquid metal is contained in a cooled mold and then it is followed by the direct cooling of the casting (Fig. 1). In the vertical process, the crystallized ingot is being constantly lowered (Fig. 2) until it reaches the bottom of the tank, which ends the casting process.

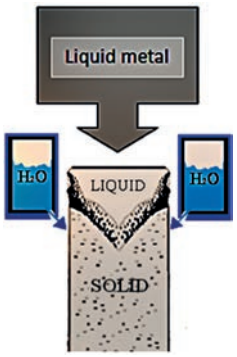

Fig. 1. Scheme of the basic DC process [10]

Rys. 1. Schemat podstawowego procesu półciągłego odlewania [10]

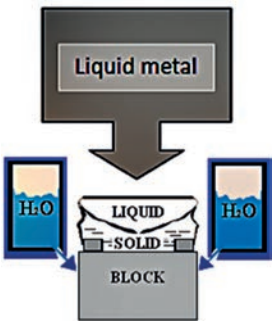

Fig. 2. First step of casting [10]

Rys. 2. Pierwszy etap odlewania [10]

Microstructure of ingots cast in the DC process is characterized by a segregation zone, coarse dendrite arm spacing (DAS), a large grain size and various other features. Such a structure explains the existence of numerous defects such as edge cracking during rolling, anodizing streaks, and back end defects in extrusions. Many of these can result in difficulties in further processing. Observation and control of ingot distortions

(Fig. 3), the changes on its surface and in its microstructure has been the basis for improving casting technology that would help to minimize defects [10].

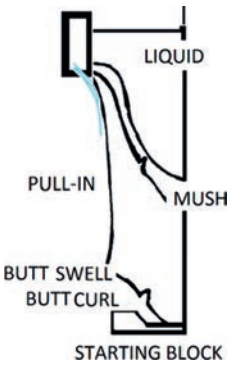

Fig. 3. A view of the ingots typical for DC-casting [9]

Rys. 3. Widok typowego wlewka otrzymanego podczas półciągłego odlewania [9]

2. The experimental details

The test was carried out on 7003, 7003S and 7010K alloys, taken from the annealed ingots. Ingots were made from Al-Zn-Mg-Cu alloy containing zirconium in the range of 0.11−0.16%. Symbols S and K are our internal modifications, still compatible with the standard. Part of the comparative research was also carried out on samples taken from the 7010 series on-annealed ingots. Both destructive and non-destructive tests were carried out.

Two slices with thickness of 25 mm were extracted from the top and bottom of ingots, coming from melting of 7003, 7003S and 7010K alloys, after homogenization. One additional 250 mm slice was cut from the middle of the ingots. The temperature at the beginning, middle and end of the casting process, for all three alloys, was about 680°C. The samples for analysis after longitudinal turning have been etched in 20% aqueous NaOH solution.

The study consisted of the analysis of the macro- and microstructure of homogenized and non-homogenized ingots. The chemical profiles of ingots have been determined using a flame spectrophotometer ARL 3460 OES. Chemical analysis in micro-areas by scanning electron microscopy with energy-dispersive X-ray spectroscopy (SEM-EDS) was performed and the distribution of chemical elements in the microstructures are also presented. The XRD (X-Ray Diffraction) method was also used to show specific phases in the alloys.

3. Results and discussion

3.1. Chemical analysis

The chemical analysis was performed using a spark spectrometer ARL 3460 OES. Three tests were carried out on the cross section of each sample: near the edge, in the middle of the cross section and in the middle of its radius.

Analysis of chemical composition is presented in Figure 4.

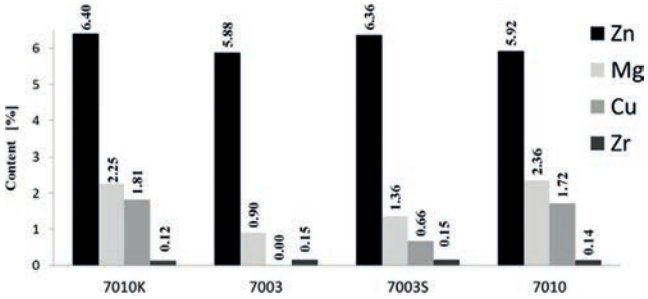

Fig. 4. Comparison of the alloying elements content (Zn, Mg, Cu, Zr) – homogenized (7010K, 7003, 7003S) and non-homogenized (7010) alloys, wt. %

Rys. 4. Porównanie zawartości podstawowych dodatków stopowych (Zn, Mg, Cu, Zr) dla stopu: homogenizowanego (7010K, 7003 i 7003S) oraz 7010 (niehomogenizowanego), % wag.

From the chemical analysis comes the observation that the density of elements content at the beginning and at the end of the ingot differs significantly. Two groups of ingots, made from 7010K and 7003S alloys contain Zn, Mg, Cu, Fe and Zr while ingots from 7003 alloy without copper and contain Zn, Mg, Fe, Mn and Zr. On the other hand, normalized 7010 alloy contained about 89.4 (wt. %), of aluminum and about 10.6 (wt. %) of additions and contaminations.

3.2. Metallographic analysis

Comparison of the results of macro- and microstructure analysis for the chosen alloys is presented in Figures 5 to 21. The grains take on a characteristic form in the ingot cooling process and their diameter increases gradually from the edge to the middle of the cross section.

It is observed in the macrostructures that the smallest precipitates are present in the 7003 alloy while the largest are in the 7003S. Larger emissions can be observed for 7003S. 7010K is characterized by clearly visible dendritic structure.

Segregation often occurs in aluminum alloys. It is connected to greater overcooling in the parts of the ingot that is closest to the cooling medium. There is also a layer being created on the ingots surface that is often called ‘skin’ (Fig. 5). It has a slightly changed chemical composition and properties – it is much tougher and the grains observed in the macrostructure are coarser.

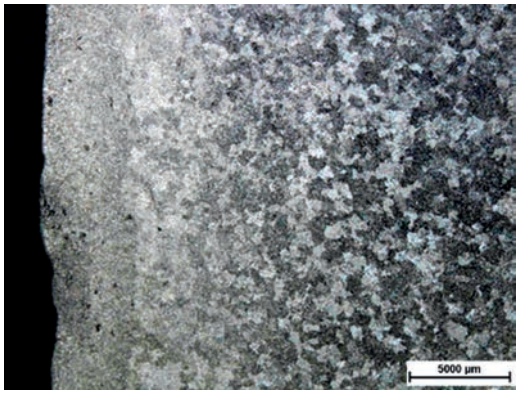

Fig. 5. Macrostructure of the cross section of the ingot made from 7010 alloy (non-homogenized sample) – ingot middle section – edge of the sample, coastal zone, high grain refinement,10×

Rys. 5. Makrostruktura na przekroju poprzecznym wlewka ze stopu 7010 (wlewek niehomogenizowany) – widoczna strefa brzegowa, bardzo rozdrobniona, 10×

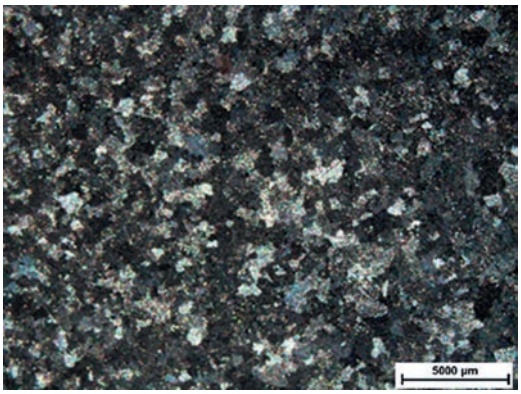

Fig. 6. Macrostructure of the cross section of the ingot made from 7010 alloy (non-homogenized sample) – half of the radius of the ingot, 10×

Rys. 6. Makrostruktura na przekroju poprzecznym wlewka ze stopu 7010 (wlewek niehomogenizowany) – połowa promienia wlewka, 10×

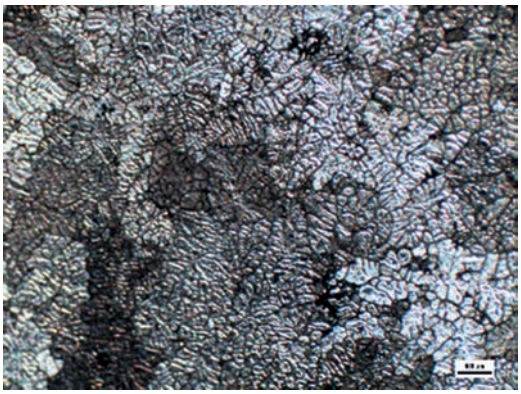

Fig. 7. Macrostructure of the cross section of the ingot from 7010 alloy (non-homogenized) – middle of ingot, 50×

Rys. 7. Makrostruktura na przekroju poprzecznym wlewka ze stopu 7010 (wlewek niehomogenizowany) – środek wlewka, 50×

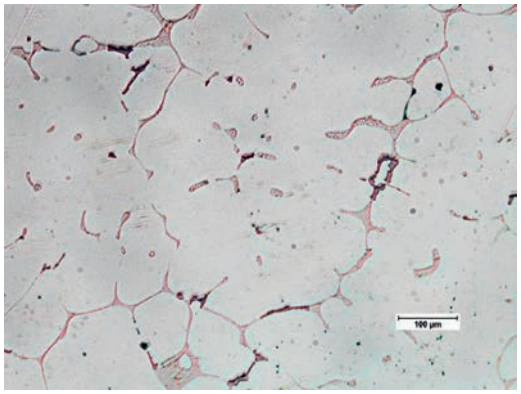

Fig. 8. Microstructure in the longitudinal section of the non-homogenized ingot from 7010 alloy, middle of ingot, 200×

Rys. 8. Mikrostruktura na przekroju podłużnym wlewka niehomogenizowanego ze stopu 7010, środek wlewka, 200×

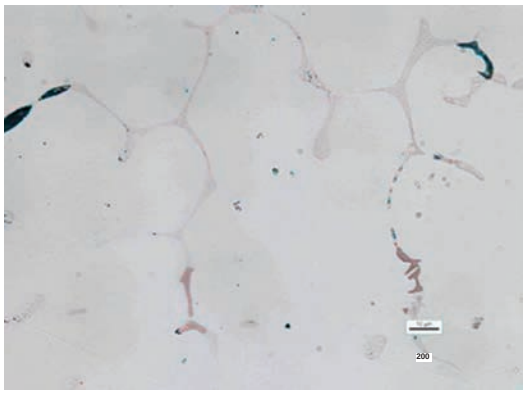

Fig. 9. Microstructure in the longitudinal section of the non-homogenized ingot from 7010 alloy, middle of ingot, 500×

Rys. 9. Mikrostruktura na przekroju podłużnym wlewka niehomogenizowanego ze stopu 7010, środek wlewka, 500×

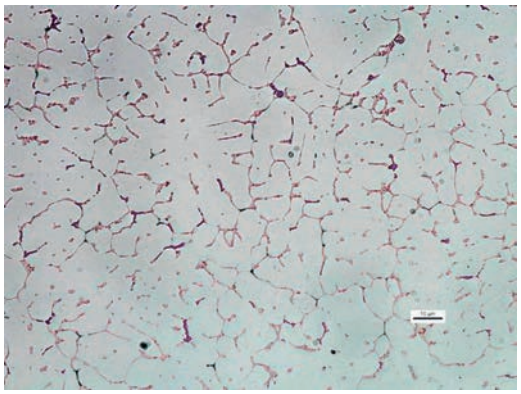

Fig. 10. Microstructure in the longitudinal section of the non-homogenized ingot from 7010 alloy, edge of ingot, 100×

Rys. 10. Mikrostruktura na przekroju podłużnym wlewka niehomogenizowanego ze stopu 7010, brzeg wlewka, 100×

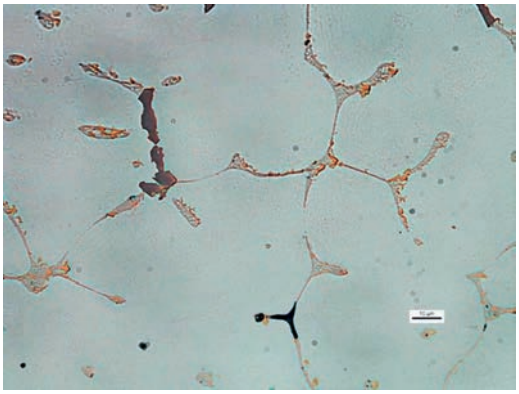

Fig. 11. Microstructure in the longitudinal section of the non-homogenized ingot from 7010 alloy, edge of ingot, 500×

Rys. 11. Mikrostruktura na przekroju podłużnym wlewka niehomogenizowanego ze stopu 7010, brzeg wlewka, 500×

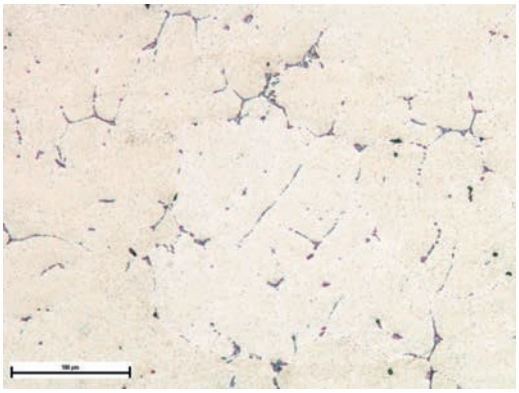

Fig. 12. Microstructure in the longitudinal section of the homogenized ingot from 7003 alloy, edge of ingot, 200×

Rys. 12. Mikrostruktura na przekroju podłużnym wlewka homogenizowanego ze stopu 7003, brzeg wlewka, 200×

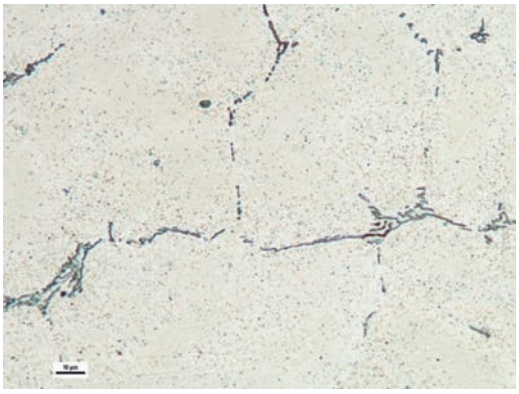

Fig. 13. Microstructure in the longitudinal section of the homogenized ingot from 7003 alloy, edge of ingot, 500×

Rys. 13. Mikrostruktura na przekroju podłużnym wlewka homogenizowanego ze stopu 7003, brzeg wlewka, 500×

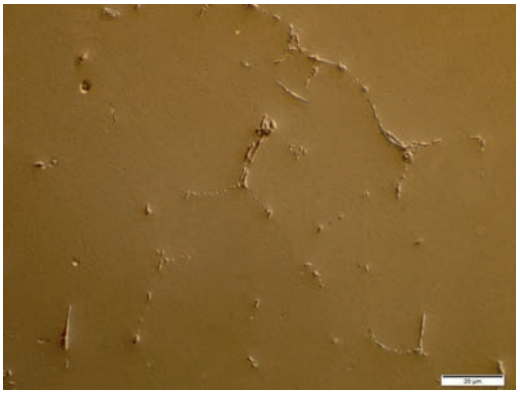

Fig. 14. Microstructure of the cross section of the homogenized ingot from 7003 alloy, middle of ingot, 1000×

Rys. 14. Mikrostruktura na przekroju poprzecznym wlewka homogenizowanego ze stopu 7003, środek wlewka, 1000×

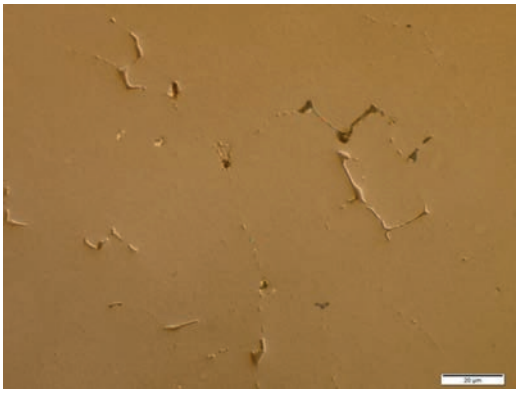

Fig. 15. Microstructure of the cross section of the homogenized ingot from 7003S alloy, middle of ingot, 1000×

Rys. 15. Mikrostruktura na przekroju poprzecznym wlewka homogenizowanego ze stopu 7003S, środek wlewka, 1000×

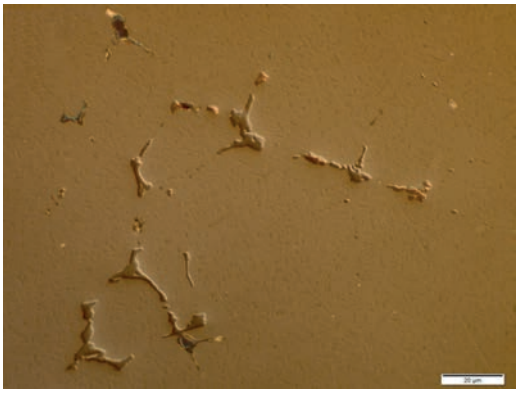

Fig. 16. Microstructure of the cross section of the homogenized ingot from 7010K alloy, middle of ingot, 1000×

Rys. 16. Mikrostruktura na przekroju poprzecznym wlewka homogenizowanego ze stopu 7010K, środek wlewka, 1000×

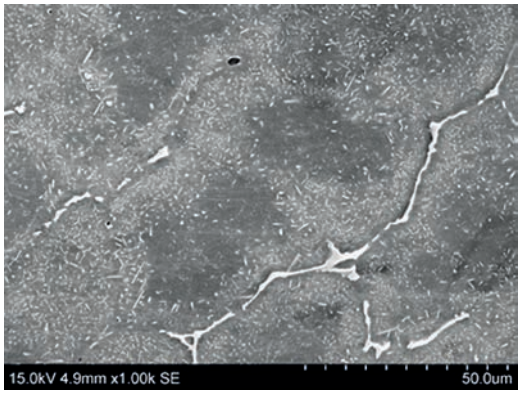

Fig. 17. Microstructure of the cross section of the homogenized ingot from 7003S alloy, 1000×

Rys. 17. Mikrostruktura na przekroju poprzecznym wlewka homogenizowanego ze stopu 7003S, 1000×

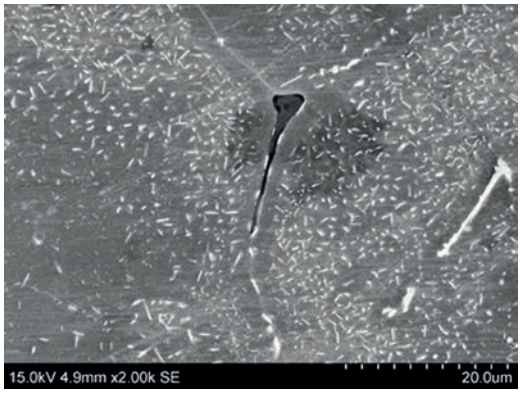

Fig. 18. Microstructure of the cross section of the homogenized ingot from 7003S alloy, 2000×

Rys. 18. Mikrostruktura na przekroju poprzecznym wlewka homogenizowanego ze stopu 7003S, 2000×

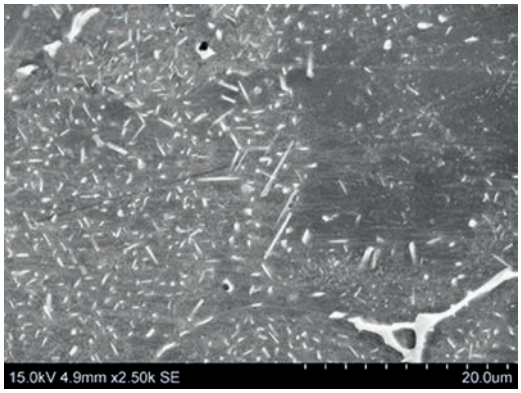

Fig. 19. Microstructure of the cross section of the homogenized ingot from 7003S alloy, 2500×

Rys. 19. Mikrostruktura na przekroju poprzecznym wlewka homogenizowanego ze stopu 7003S, 2500×

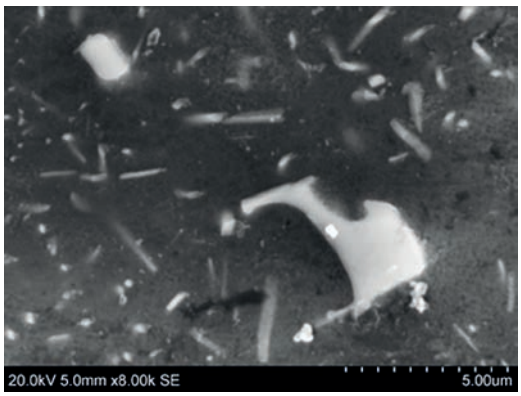

Fig. 20. Microstructure of the homogenized ingot from 7003S alloy, 8000×

Rys. 20. Mikrostruktura wlewka homogenizowanego ze stopu 7003S, 8000×

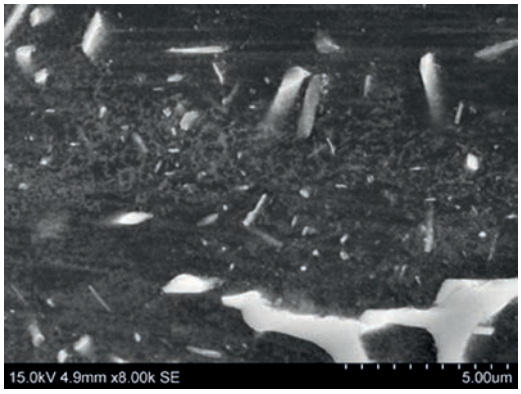

Fig. 21. Microstructure of the homogenized ingot from 7003S alloy, 8000×

Rys. 21. Mikrostruktura wlewka homogenizowanego ze stopu 7003S, 8000×

3.3. Chemical analysis of the chosen elements of micro-structural

The phases observed in Figures 17−21 and complex composition of 7003S alloy both suggest a diverse chemical composition in the micro scale as well. The test material was also analyzed from the point of view of quality and quantity, the elements included in the chemical composition of the material in the micro scale (Fig. 22).

In Figures 23−25, the distribution of elements in microstructure of the 7003S alloy are presented. The publication includes XRD spectra's that show which specific phases are present in the alloys. That has been achieved by using XRD analysis for 7003, 7003S and 7010K alloys (Figs. 26−28).

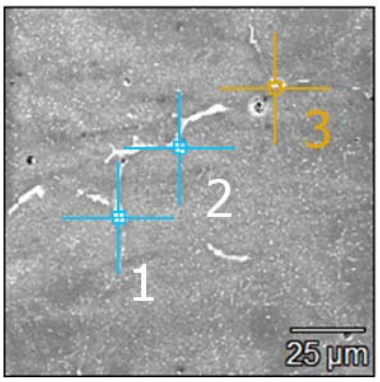

No.	Mg	Al	Si	Ca	Fe	Ni	Cu	Zn	Zr
1	0.64	61.02	-	-	28.11	0.31	6.33	3.55	0.05
2	0.96	69.94	0.12	-	18.53	-	4.90	5.55	-
3	2.93	84.39	-	0.41	-	-	2.00	10.28	-

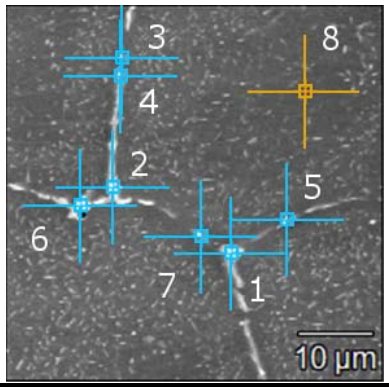

No.	Mg	Al	Si	Fe	Ni	Cu	Zn
1	1.05	70.47	-	19.19	-	4.79	4.49
2	0.85	74.44	-	16.18	-	3.99	4.55
3	9.04	79.08	5.20	0.39	-	0.86	5.42
4	5.17	65.87	-	0.68	-	2.99	25.28
5	5.88	64.91	-	-	-	3.16	26.04
6	0.92	65.33	-	24.01	0.27	5.86	3.62
7	3.26	71.28	-	0.99	-	2.71	21.76
8	1.38	89.51	-	-	-	0.85	8.27

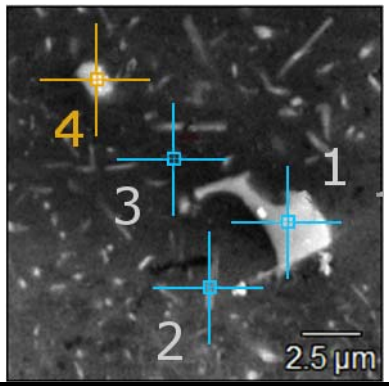

No.	Mg	Al	Si	Cr	Fe	Ni	Cu	Zn
1	0.56	65.48	2.34	0.14	23.55	0.34	4.33	3.25
2	2.18	83.75	-	-	-	-	1.19	12.88
3	1.02	91.01	-	-	0.23	-	0.74	7.01
4	1.58	89.70	-	-	0.66	-	0.82	7.24

Fig. 22. The chemical composition for the selected measuring points for the 7003S alloy, wt. %

Rys. 22. Skład chemiczny w mikroobszarach dla próby ze stopu 7003S z zaznaczonymi punktami pomiarowymi, % wag.

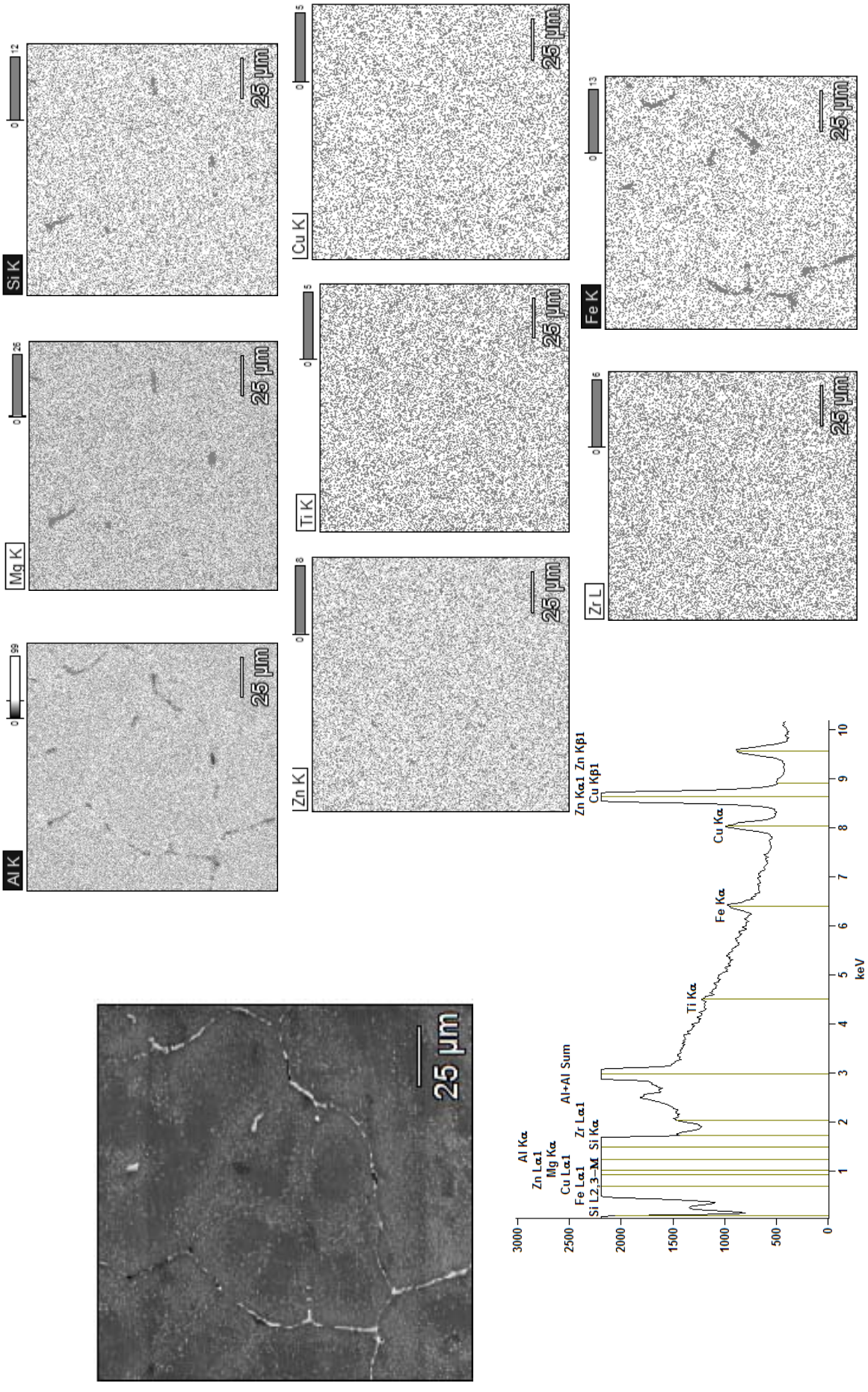

Fig. 23. Micro-structural analysis with scanning electron microscope with included EDS for 7003S series aluminum alloy

Rys. 23. Analiza mikrostruktury przy użyciu skaningowego mikroskopu elektronowego z analizą SEM dla stopu aluminium serii 7003S

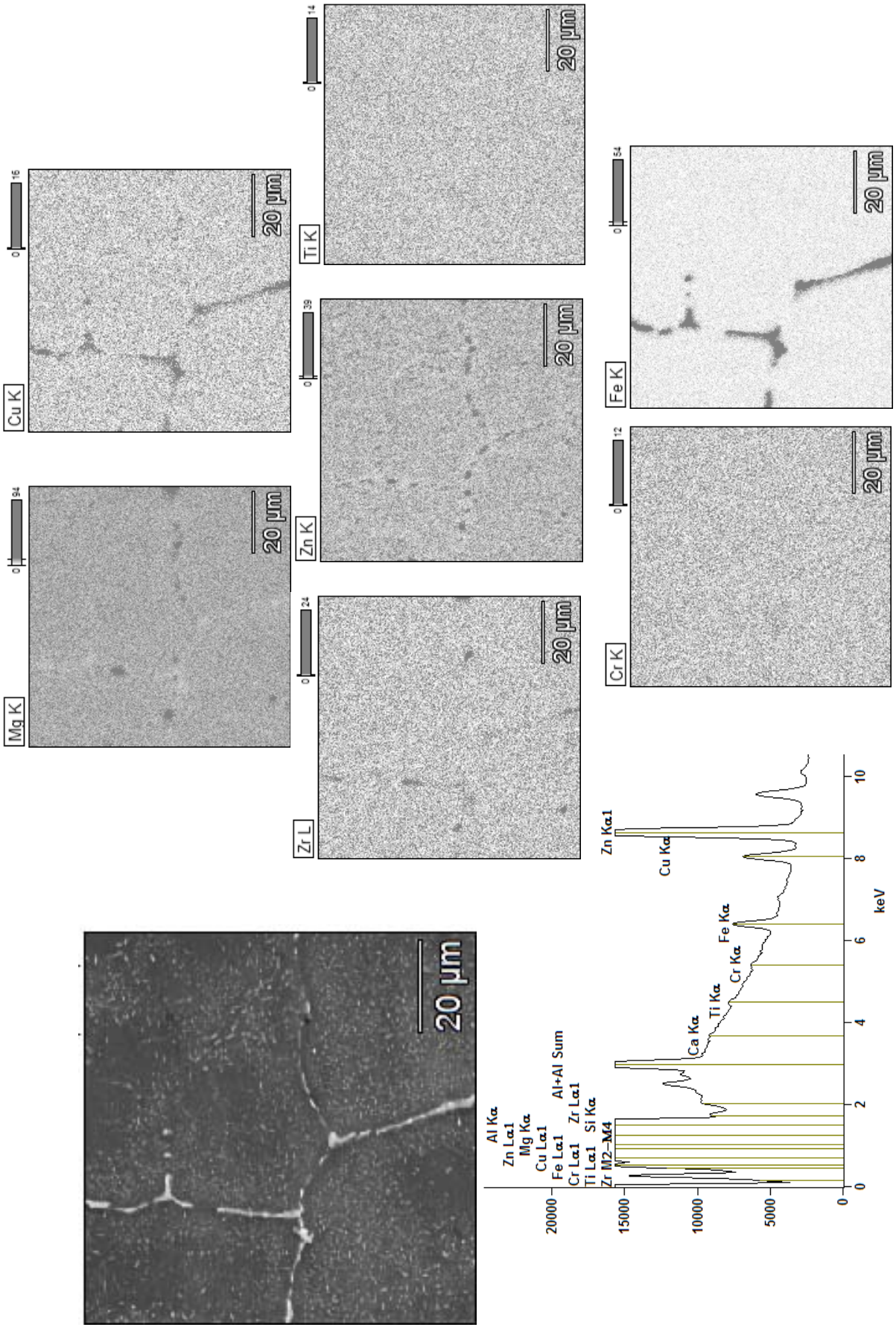

Fig. 24. Micro-structural analysis with scanning electron microscope with included EDS for 7003S series aluminum alloy

Rys. 24. Analiza mikrostruktury przy użyciu skaningowego mikroskopu elektronowego z analizą SEM dla stopu aluminium serii 7003S

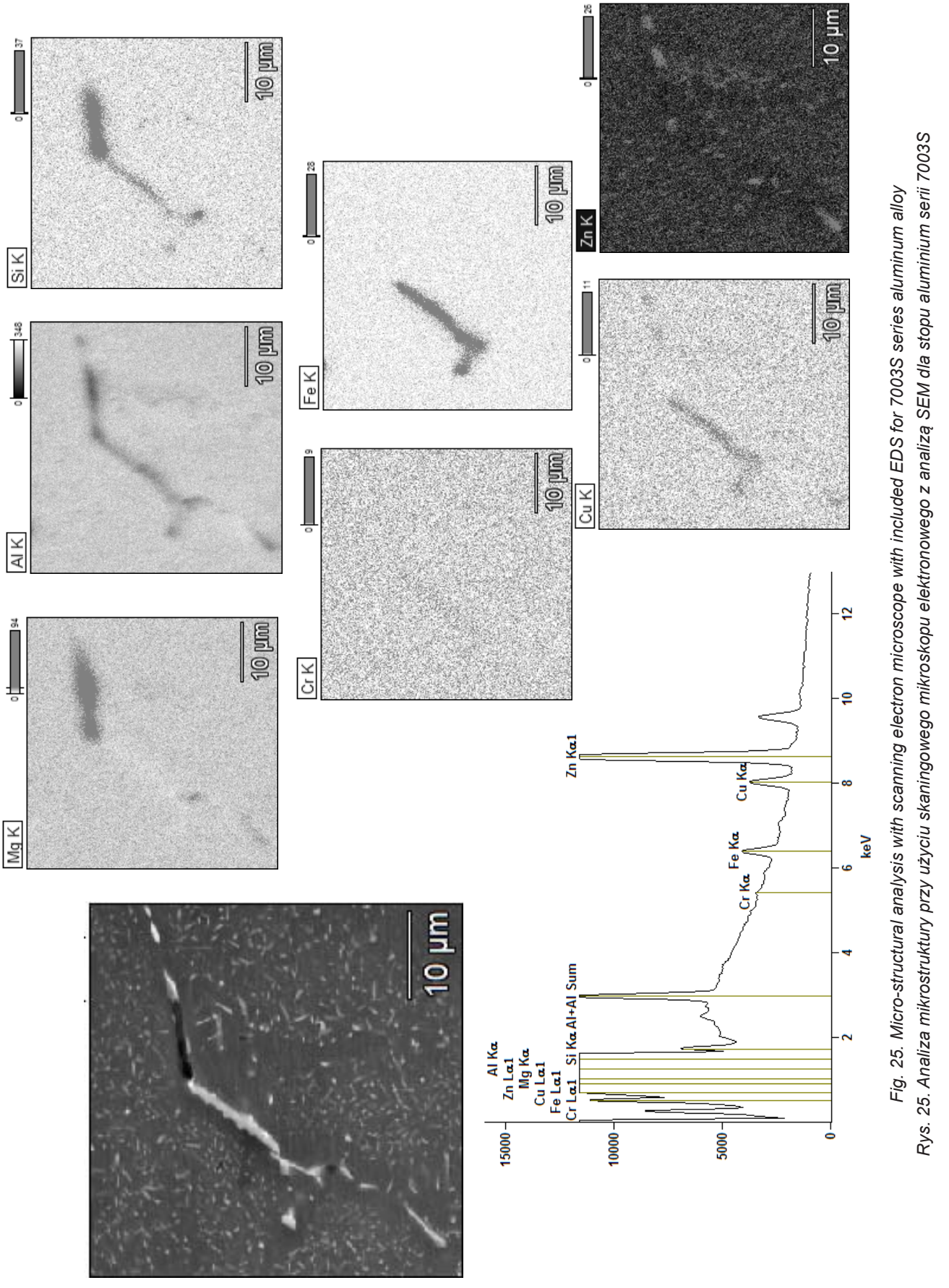

Fig. 25. Micro-structural analysis with scanning electron microscope with included EDS for 7003S series aluminum alloy

Rys. 25. Analiza mikrostruktury przy użyciu skaningowego mikroskopu elektronowego z analizą SEM dla stopu aluminium serii 7003S

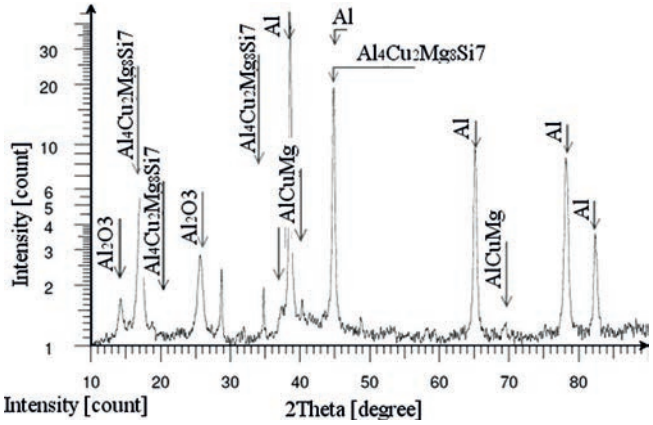

Fig. 26. X-Ray Diffraction for 7003 series aluminum alloy
Rys. 26. Dyfrakcja rentgenowska XRD dla stopu 7003

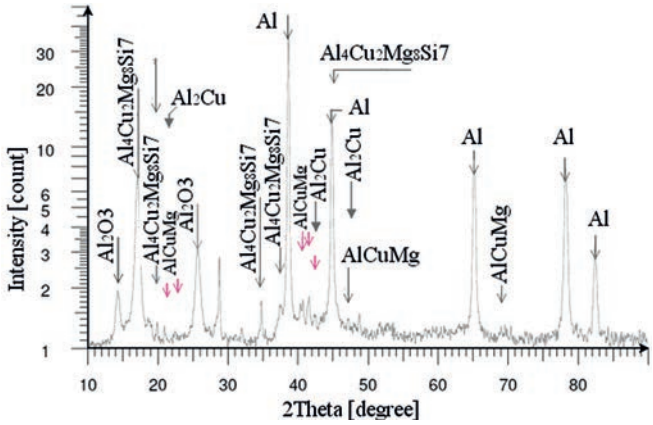

Fig. 27. X-Ray Diffraction for 7003S series aluminum alloy
Rys. 27. Dyfrakcja rentgenowska XRD dla stopu 7003S

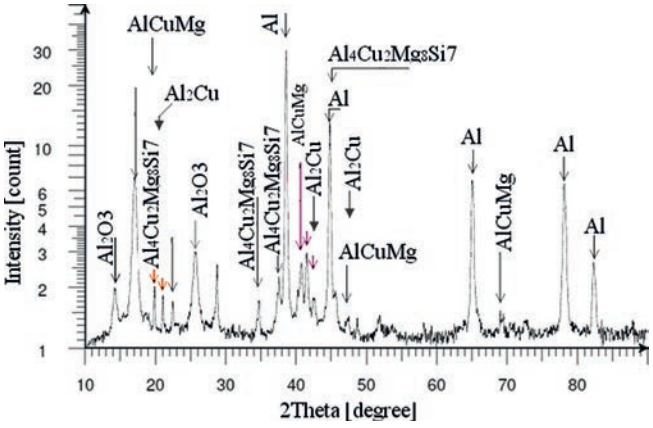

Fig. 28. X-Ray Diffraction for 7010K series aluminum alloy
Rys. 28. Dyfrakcja rentgenowska XRD dla stopu 7010K

SEM-EDS analysis for 7003S alloy shows that bright emissions on the grain edges contain approximately 63% Al, 24% Fe, 6% Cu and 4% Zn. Dark regions in the microstructures are aluminum-rich with around 7% Zn and small amounts of Cu additions. Rhomboid emissions contain high concentrations of zirconium, around 22% and magnesium, around 3%. On the grain boundaries high concentrations of iron, copper, and zirconium is visible but there is much less magnesium. On the other hand, regions containing more magnesium have more copper and much less iron.

Chemical analysis of the microstructure for 7003S alloy has been confirmed by the EDS analysis. On the grain edges there is Al together with Fe, Mg and Si. Light phases are iron-rich and in addition contain Al, Cu and Zn. Analysis of the microstructure by EDS using a scanning electron microscope shows that magnesium occurs together with aluminum and silicon and can be seen as dark emissions on the grain edges. The X-ray diffraction charts prove that the 7003 alloy includes: $Al_4Cu_2Mg_8Si_7$, AlCuMg, Al_2O_3. It is similar for both 7003S and 7010K alloys but in addition they contain the Al_2Cu phase.

4. Conclusions

The grains are formed in a particular way during the cooling process in the crystallizer. The larger grains are in the middle of the ingot and have larger diameters, which can be observed in the microstructures. The smallest grains are visible for 7003 alloy. 7010K alloy has a highly dendritic structure. Semi-continuous casting together with homogenization enables the production of ingots with uniform cross sections as can be seen in the results of the chemical analysis.

Numerous phases inside grains existing in the solid solution, in the future can become the basis for precipitation hardening. In the case of 7003 alloy those phases are: $Al_4Cu_2Mg_8Si_7$, AlCuMg, Al_2O_3 and for 7003S and 7010K alloys they are $Al_4Cu_2Mg_8Si_7$, AlCuMg, Al_2O_3 and Al_2Cu. For 7003S alloy the above results were confirmed by the analysis with a scanning electron microscope with EDS.

Acknowledgements

Sincere thanks go to Stanislaw Rzadkosz, Prof. AGH, for a huge amount of work put into the preparation of Zofia Kwak to the subject of aluminum alloys. The results presented in this publication were partially based on research conducted under PhD thesis.

The authors wish to thank the following persons for their help in carrying out the studies: Marek Marcisz, Waldemar Krok and Grzegorz Mrowiec – Staff members in the Grupa Kęty SA in Kęty.

The authors wish to thank also for Prof. Jerzy Józef Sobczak for the possibility of publishing.

References/Literatura

1. Kwak Z., S. Rzadkosz, A. Garbacz-Klempka, W. Krok. 2014. „Wpływ dodatków stopowych na mikrostrukturę i właściwości stopów serii 7xxx". *Archives of Foundry Engineering* 14 (sp.is. 4) : 83−88.
2. Kwak Z., A. Garbacz-Klempka. 2016. Wysokowytrzymałe stopy aluminium serii 7xxx kształtowane dodatkami stopowymi. W *Monografia Tygiel 2016* (in print).
3. Kwak Z., S. Rzadkosz, A. Garbacz-Klempka, M. Perek-Nowak, W. Krok. 2015. „The properties of 7xxx series alloys formed by alloying additions". *Archives of Foundry Engineering* 15 (2) : 59−64.
4. Eivani A.R., A. Zhou, J. Duszczyk. 2011. Microstructural evolution during the homogenization of Al-Zn-Mg aluminium alloys. W *Recent Trends in Processing and Degradation of Aluminium Alloys*, 477−516. Ed. Zaki Ahmad. Rijeka: InTech Europe. Downloaded from: http://www.intechopen.com/books/recenttrends-in-processing-and-degradation-of-aluminium-alloys/microstructural-evolution-during-thehomogenization-of-al-zn-mg-aluminum-alloys [access: 26.03.2016].
5. Suenger S., M. Kreissle, M. Kahnert, M.F. Zaeh. 2014. „Influence of Process Temperature on Hardness of Friction Stir Welded High Strength Aluminum Alloys for Aerospace Applications". *Procedia CIRP* 24 : 120−124. DOI:10.1016/j.procir.2014.07.141.
6. Naeem H.T., K.S. Mohammad, K.R. Ahmad. 2014. „The Effect of Microalloying of Nickel. RRA Treatment on Microstructure and Mechanical Properties for High Strength Aluminum Alloy". *Advanced Materials Research* 925 : 253−257. DOI: 10.4028/www.scientific.net/AMR.925.253.
7. Sawicki J., Ł. Kaczmarek, W. Staszewski, J. Zgraja, P. Kędzierski, R. Kaszewski. 2009. „Przesycanie grzaniem indukcyjnym stopu aluminium 7075". *Tribologia* 6 : 103−110.
8. http://www.edinformatics.com/math_science/periodic_table_of_elements/aluminum.htm [access: 8.03.2016].
9. Eskin D.G. 2008. *Physical metallurgy of direct chill casting of aluminium alloys*. Boca Raton, London, New York : CRC Press Taylor & Francis Group.
10. Grandfield J.F., P.T. McGlade. 1996. „DC Casting of Aluminium: Process Behaviour and Technology". *Materials forum-rushcutters bay*, 20 : 29−51. Downloaded from: http://www.thaiminhiejc.com/upload/files/casting1(1).pdf [access: 26.03.2016].
11. Sanders R.E., Jr. 2001. „Technology Innovation in Aluminum Products". *JOM* 53 (2) : 21−25.